CANDIDATE'S DECLARATION

I hereby declare that the work, which is being presented in the dissertation entitled **"Dynamic Modeling of Membrane Reactor Producing Hydrogen from Steam Reforming"** in the partial fulfillment of the requirements of the award of the Degree of Master of Technology in Chemical Engineering with specialization in "Computer Aided Process Plant Design**"**, submitted in the Department of Chemical Engineering, Indian Institute of Technology Roorkee, Roorkee, is an authentic record of my own work carried out during the period from June 2012 to June 2013 under guidance of **Dr. Ravindra Bhargava**, Associate Professor, Department of Chemical Engineering, Indian Institute of Technology Roorkee, Roorkee.

I have not submitted the matter, embodied in this dissertation for the award of any other degree.

Date: June, 2013

Place: Roorkee (Shakti Priyadarshan)

Certificate

This is to certify that the above statement made by the candidate is correct to the best of my knowledge and belief.

Dr. Ravindra Bhargava
Associate Professor
Department of Chemical Engineering
Indian Institute of Technology Roorkee
Roorkee - 247667 (India)

ACKNOWLEDGEMENT

I express my deep sense of gratitude to my guide **Dr. Ravindra Bhargava**, Associate Professor, Department of Chemical Engineering, Indian Institute of Technology Roorkee, Roorkee, for his keen guidance, constant interest and encouragement throughout the course of this work, his experience, dhoon and deep insight of the subject held this work always on a smooth and steady course.

Thanks to Dr. V.K. Agarwal , Professor and Head, Department of Chemical Engineering, Indian Institute of Technology Roorkee, for providing various facilities during this dissertation. Above all, I want to express my heartiest gratitude to my parents for their love, faith and support for me, which has always been a constant source of inspiration. I also like to thank my batch mates and friends specially Prakhar Jaiswal and Vaibhav Manthalkar for their constant motivation and support.

SHAKTI PRIYADARSHAN

Abstract

A mathematical model for reformer reactor with membrane reactor that is composed of two channels separated by membrane is developed for methane steam reforming. Steam reforming takes place in reformer on a $Ni/MgO–Al_2O_3$ catalyst layer and required product, hydrogen, passes through the membrane layer. The combination of highly endothermic reforming reaction and mildly exothermic shift reaction takes place in main body of reactor which leads to continuous temperature drop through the length of reactor. To maintain the temperature of reactor, feed is preheated. Selective permeation of hydrogen through the palladium membrane is achieved by co-current flow of sweep gas through the second channel. The mass and energy balance equations for the thermally coupled membrane reactor form a set of 13 coupled partial differential equations. With the application of appropriate boundary conditions, the distributed dynamic reactor model is solved as a boundary value problem. The model equations are discretized using forward difference method on finite elements. The discretized nonlinear modeling equations, along with the boundary conditions, form a system of algebraic equations that are solved in C++. The performance of the reactor is numerically investigated for various key operating variables such as inlet fuel concentration, inlet steam/methane ratio, inlet reformer gas temperature and inlet reformer gas velocity. For each case, the reactor performance is analyzed based on methane conversion and hydrogen recovery yield.

Table of Content

NOMENCLATURES

C	Concentration, kmol/m^3
C_p	Heat capacity, j/kg K
D	Hydraulic diameter, m
E_p	Activation energy, j/kmol
H	Enthalpy, j/kmol
ΔH	Heat of reaction, j/kmol
ΔH_{298}	Heat of reaction at 298 k, j/kmol
$h_{r,m}$	Heat transfer coefficient between sweep gas and reformer, w/m^2K
$h_{r,w}$	Reformer–wall heat transfer coefficient, w/m^2K
J	Hydrogen permeation flux, kmol/m^2 s
k_1, k_3	Reaction rate constant for I and III reaction, kmol $Pa^{1/2}$kg cat/hr
k_2	rate coefficient of reaction II, kmol/kg cat.h.Pa
K	Equilibrium constant
P	Partial pressure, Pa
P	Total pressure, Pa
Q_0	Pre-exponential factor, kmol/m$Pa^{1/2}$ s
R_g	Gas constant, j/kmolK
R	Rate of generation, kmol/s-kg of catalyst
S_m	Hydrogen permeation area per unit volume of Sweep gas channel, 16.5m^2/m^3
T	Thickness, m

T	Temperature, K
U	Velocity, m/s
Z	Length of the reactor, m

SYMBOLS

ρ	density, kg/m^3
t	Membrane thickness, m
H	effectiveness factor
λ	thermal conductivity, W/m K
E	reformer bed porosity

SUBSCRIPTS

E	Reaction
i	i^{th} Reactant
j	j^{th} Reaction
m	Sweep gas
R	Reformer
Ref	Reference
W	Reactor wall

Tables

List of Figures

1 Introduction

Steam reforming

Steam reforming of methane is the most common method of producing commercial bulk hydrogen and produced hydrogen is industrially used in ammonia synthesis. It is the cheapest method of hydrogen generation at high temperatures (in the range of 700 to 1100 °C) and in the presence of a metal-based catalyst. Steam reforming process is the set of two reactions – reforming reaction and water gas shift reaction.

- Reforming reaction - methane reacts with steam to form carbon monoxide and hydrogen.

$$CH_4 + H_2O \rightarrow CO + 3\ H_2$$

This reaction is highly endothermic which require 206 kJ/mol of heat

- Shift reaction – Carbon mono oxide formed in reforming reaction combines with steam to form hydrogen and carbon dioxide.

$$CO + H_2O \rightarrow CO_2 + H_2$$

Shift reaction is mildly exothermic in nature releasing 41 kJ/mol.

The product hydrogen of reforming has great importance in industries. Hydrogen is used to increase the performance of petroleum products in petroleum refineries by removing organic sulfur from crude oil as well as to convert heavy crude oil to easier to refine, lighter and more marketable product. Moreover hydrogen has its great importance in terms of meeting Clean Air Act requirements.

Apart from petroleum hydrogen has its greater demand in fertilizer industries and for fuel cell application.

Efficiency of steam reforming process varies from 65% to 75 % and to improve this two methods can be coupled with the process which are summarized as follows

- Membrane assisted with the coupled reactor**:** From Le Chatelier's principle in thermodynamics, continues removal of any product from the reaction mixture increase the rate of forward reaction hydrogen removal through palladium membrane in increase the hydrogen yield in the process.

In the present work, steam reforming of methane is investigated in a tubular reactor with membrane. The study is done for unsteady state case. The dynamic model of tubular reactor having membrane is presented and effects of various operating parameters like inlet gas velocity, methane to steam ratio, thickness and type of membrane, temperature of preheated reactant, effect of sweep gas, change in temperature along the length of reactor, city are numerically investigated. For these operating variables, the reactor performance is analyzed based on methane conversion and hydrogen recovery yield.

Problem description:

A preheated mixture of natural gas (methane) and steam undergoes in a flat parallel geometry where it reacts in the presence of catalyst to from hydrogen and carbon monoxide meanwhile product carbon monoxide reacts with steam to further form hydrogen and carbon dioxide. First reaction, called steam reforming occurs endothermally and second, water gas shift reaction exothermally. Reforming reaction is highly endothermic and shift reaction is lightly endothermic. The combination of opposite nature reactions leads to overall highly endothermic reaction resulting to temperature drop in the reactor along the length of reactor as reactions proceed. Both reversible reactions are controlled by the concentrations of product. This tubular

reactor is covered by a thin layer of membrane and reaction is occurring in the presence of metal based catalyst accompanied by membrane. The use of membrane helps to selectively separate one of the products, hydrogen; shifting the equilibrium in the forward direction leading to enhancement in the net rate of production of hydrogen. For better permeation of hydrogen through membrane nitrogen is used as a sweep gas. For recovery of pure hydrogen, gaseous mixture from sweep gas channel is further processed, which is out of scope of this study. The dynamic model of reactor is presented afore and influence of different operating parameters e.g. inlet gas temperature, reactant ratio, reactant velocity, thickness of membrane, type of catalyst etc. is computed numerically. For above parameters, performance of reactor is monitored numerically on the basis of H_2 yield and methane conversion.

In view of the above, the present work is compiled in following chapters wherein,

Chapter 1, Introduction

Chapter 2, presents an overview of various literatures related to this study.

Chapter 4, contains development of all modeling equations used in this model.

Chapter 5, illustrates the method used to simulate the model.

Chapter 6, Results,

Chapter 7, Conclusions and future work.

Chapter 8, References.

2 Literature Review

2.1 Literature reviews for Membrane reactor

Shu et al., (1994): For steam reforming reactions they applied asymmetric Pd- and Pd-Ag/ porous SS membrane reactors. The conversion of methane was raised by partial removal of hydrogen from reactor. Hydrogen diffused through Pd based membrane. They manufactured Pd-Ag/porous stainless steel composite membrane by electrolessly deposition. Methane Conversion was increased twice at the total reactor pressure of 136 kPa, 500°C temperature and methane content in feed was taken 30% of steam, when membrane was used with the combination of commercial Ni/Al_2O_3 catalyst with Pd/SS membrane. The effects of feed ratio, feed velocity, feed temperature, membrane efficiency etc. were tested experimentally. For the prediction of effects of membrane on fuel conversion, they developed computer model. They developed the relation for hydrogen permeation rate in palladium membrane.

Barbieri et al., (1997) used parallel-flow and counterflow configurations for the simulation of reactors to study the methane steam re-forming reaction in a packed-bed inert membrane reactor (PBIMR). This study also concluded to the complete conversion of methane is possible with total hydrogen removal from reaction products. Simulation used an infinite hydrogen permselective dense Pd membrane in the mode. They compared membrane reactor performance with that of a conventional fixed-bed reactor and they analyzed the effect on the degree of conversion for different parameters such as temperature, reactor pressure, feed and sweep flow rate, feed molar ratio, membrane thickness, and space velocity. They compared experimental

data with data of Shu et. al. (1994) and showed a good agreement. The result analysis indicates that the choice of operating conditions requires a complex process strategy.

Lin et al., (2003) studied, experimentally and by modeling, the effects of incipient removal of hydrogen through palladium membrane on the conversion of methane steam reforming. To describe the displacement of methane conversion in the steam reforming, they presented a mathematical model based on the reaction rate expressions. They examined influence of different parameters mainly "weight hourly space velocity" (WHSV), surface-to-load ratio, reaction Temp-Pressure, composition (partial pressure) of hydrogen in upstream side (permeate side) and reaction temperature. Their study, simulation and experimental results showed that a conversion level more than 80% was reached in a palladium membrane reactor operating at 500°C which is equivalent conversion that could be accomplish at 850°C in a FBR. In addition to this, the Carbon monoxide yield was very low compared to FBR, less than two percent for MR and upto 50 % in FBR. This shows the usefulness of MR compared to any other set conventional hydrogen producing method and reactor type.

Chen et al., (2003) examined the performance of an ideal fast fluidized bed membrane reactor (CFFB-MR) using a mathematical model. Type of reactor was circulating FBR The produced H_2 was removed with the use of permselective membranes. Membrane was also considered ideal, shifting thermodynamic equilibrium toward forward reaction direction. So the higher conversion was reached at a relatively lower temperature. The reaction was integrated with methane combustion supplying require heat for reforming reaction. The integration with of

the exothermic reforming and steam reforming continuously forms hydrogen with high yield without lowering the temperature eliminating use of any external heat source for preheating the feed and maintains the constant temperature within the reactor. The simulation results give that the H_2 productivity (moles H_2 produced/hour per unit reactor volume) of considered reactor is 8 times that in industrial FBR and 112 times than in a BFB-MR.

Sun et al., (2004) focused their study mainly on influence of catalyst on hydrogen production from ethanol. The approach was to develop hydrogen producing model for fuel cell application therefore at low temperature range with high yield of hydrogen. For high yield at low temperature, they used Y_2O_3 supporting Ni nano-particles. This gave 98% ethanol conversion at about 300^0C while CeO_2/ZrO_2 results same at 500^0C. Further increase of temperature give 100% conversion at 500^0C with Ni/Y_2O_3.

Tsuru et al., (2004) investigated SRM, theoretically considering microporous membranes. They conducted study with O_2 and again without O_2, and studied the effect of presence of O_2. They considered microporos membrane made of silica which not only permeate H_2 but also other gaseous products. They verified their model results with experimental studies. They modeled and simulated catalytic membrane reactor with a concurrent flow pattern, with the assumption of isothermal reactor and PF type reactor with the small amount of H_2 removal through barrier. They used two unitless numbers, the Damkohler no (Da) and the Permeation no (θ) to observe the effect of operating conditions on CH_4 conversion and H_2 production. Permeation number has almost same effect of CH_4, X_{CH4} in the connection of the retention ratios of H_2 over N_2, and H_2 purity in the permeate increased as more H_2 selective barrier is introduced. Silica microporous

layer and a Ni-catalyst layer is used as catalytic membrane. A wide variation, from one to 20, in the permeability ratio of H_2 to H_2O was noticed for different operating conditions. By extracting H_2 in outer side, CH_4 conversion, X_{CH4} reached up to approximately 0.8 beyond the equilibrium conversion of 0.44

Gallucci et al., (2004) investigated the effect of different parameters on methane conversion taking methane steam reforming reaction from a modeling viewpoint. Considering the influence of the lumen pressure on methane conversion at constant temperature, they found that increasing the lumen pressure, equilibrium methane conversion increases for the membrane reactor, while it decreases for the traditional one, for example. On the other hand, in a realistic membrane reactor (i.e. considering a simulation performed using kinetic expressions), the behavior of methane conversion versus lumen pressure at various temperatures showed a minimum value. This minima depends on the membrane thickness, reactor length and on the reactor temperature.

Borgognoni et al.,(2011) conducted various experiments with different membrane geometries and did a comparative study of these geometries with fluidized bed reactor and monitored the effect of shape and structure of membrane on overall conversion and hydrogen yield. Hydrogen was synthesized by methane and effects of reaction parameters were sampled.

2.2 Methane steam reforming

Froment et al., (1989) consider a larger number of detailed reaction mechanisms and derived intrinsic rate equations for the steam reforming of methane, accompanied by water-gas

shift on a $Ni/MgAl_2O_4$ catalyst. Thermodynamic analysis used to reduce the number of possible mechanisms. They retained twenty one sets of three rate equations and subjected them to parameter estimation and model discrimination. The solution of these rate equations estimate the best model and are statistically significant and thermodynamically consistent.

They developed kinetic expression for reforming reaction, shift reaction and combined reaction are given by

$$R_1 = \frac{1}{(DEN)^2}\frac{k_1}{{P_{H2}}^{2.5}}\left(P_{CH4}.P_{H2O} - \frac{{P^3}_{H2}.P_{CO}}{K_1}\right)$$

$$R_2 = \frac{1}{(DEN)^2}\frac{k_2}{{P_{H2}}^{3.5}}\left(P_{CH4}.{P^2}_{H2O} - \frac{{P^4}_{H2}.P_{CO2}}{K_2}\right)$$

$$R_3 = \frac{1}{(DEN)^2}\frac{k_3}{P_{H2}}\left(P_{CO}.P_{H2O} - \frac{P_{H2}.P_{CO2}}{K_3}\right)$$

$k_1 = 9.048*10^{11}*\exp(-209500/R_gT)$

$k_2 = 5.43*10^{5}*\exp(-70200/R_gT)$

$k_3 = 2.14*10^{9}*\exp(-211500/R_gT)$

$K_1 = 5.75*10^{12}*\exp(-95616.31415/RgT)$

$K_2 = 1.26*10^{-2}*\exp(38246.52566/RgT)$

$K_3 = 7.24*10^{10}*\exp(-178769.9352/RgT)$

$K_{CH4} = 1.995*10^{-3}*\exp(36650/R_gT)$

$K_{H2} = 8.11*10^{-5}*\exp(70230/R_gT)$

$K_{CO} = 7.05*10^{-9}*\exp(686358.8464/RgT)$

$K_{H2O} = 1.68*10^{4}*\exp(-85770/R_gT)$

Table 2.1 Parameters of Langmuir Hinshelwood Model

T(K)	k_1	K_{CH4}	K_{O2}
663	995.94	$1.12*10^{-2}$	1.405
713	1058.20	$2.87*10^{-2}$	4.898
723	1313.92	$5.896*10^{-2}$	13.594
E_a (kJ/mol)	34.17	-	-

Rosa et al., (2001) used catalyst of large pore size to model the methane steam reforming reactor. Methane steam reforming is an endothermic process requiring high quantities of heat. Catalysts with low effectiveness factors they promoted intraparticle forced convention by use of large-pore structured catalysts, in order to reduce intraparticle gradients. Low intraparticle gradient leads to increased efficiency of the process. In the steady-state regime, in order to evaluate the effect of this convective phenomenon, they analyzed three reactor models (two dimensional and one-dimensional models): the pseudo-homogeneous model (*PH*), the heterogeneous model which considers diffusions as the only mechanism of transport inside the solid (HT_d) and the heterogeneous model which also including the intraparticle convection (HT_{dc}). Moreover, they calculated wall temperatures that must be used for getting the same final conversion of methane through the two heterogeneous models.

Gallucci et. al.,(2006) investigated steam reforming of methane from modeling viewpoint and compared the model results with industrial data. They considered the effect of different

operating parameters in overall conversion of methane and hydrogen yield. They mainly focused on flow mode of sweep gas and its type. They compared the results of membrane reactor with traditional non membrane ones.

Patel and Sunol (2007) introduced a mathematical model of a reactor divided in three channels. The concept was heat integrated membrane reactor, supplying the required heat for endothermic reforming reaction by burning of CH_4 is outer most layer of concentric cylindrical reactor. The catalyst used for combustion is arranged in very thin layer to provide minimum heat transfer resistance. They also compared the flow pattern and concluded with favoring of counter flow of sweep gas in reactor. His result showed the complete conversion of methane was possible with proper choice of operating parameters and flow patterns.

Wang et al. (2009) produced hydrogen by steam reforming of ethanol under the condition of cold plasma using the theory of density function and studied the thermodynamics of process. Hydrogen was produced from combustion of H^*, $CH_3{}^*$ and $CH_3CH_2{}^*$ ions.

Halabi et al., (2010) presented the intrinsic kinetics of methane steam reforming developed over $Rh/Ce_{0.6}Zr_{0.4}O_2$ catalyst in a relatively low temperature range of 475-375^oC and 1.5 bar pressure. They conducted kinetic experiments in an integral fixed bed reactor with no mass and heat transfer limitations and far from equilibrium conditions. Therefore, they guaranteed intrinsic reaction rate measurements. The model is based upon two-site adsorption surface hypothesis and 14 elementary reaction steps are postulated, CH_4 is dissociatively adsorbed onto the Rh active

site, and H_2O is adsorbed on the Ceria support active sites. The thing which come over was, there was no competition between CH_4 and H_2O in adsorbing on the same site. The kinetic rate expressions are according to the Langmuir-Hinshelwood formalism. They considered the redox surface reactions between the carbon containing species and the lattice oxygen leading to CO-CO_2 formation as the rate determining step. The model was found to be statistically accurate and thermodynamically consistent. The estimated activation energies and adsorption enthalpies were in agreement with literature for CH_4 steam reforming reaction over Rh. Reaction kinetics also validated by steam reforming experiments at 550°C and 1.5 bar with the use of 150 mg catalyst in a diluted bed of 5 cm length. They implemented the kinetic model in a one-dimensional pseudo-homogenous plug flow reactor model and thus simulated at identical experimental conditions. The simulation results in excellent agreement with the experimental values.

Rossi et. al.,(2011) developed a mathematical model of a Pd based membrane for production of hydrogen from syngas and separation of hydrogen through Pd membrane. The derived model is helpful for study of parameters like permeability of hydrogen, coverage of membrane surface and other limiting steps like steam-fuel ratio, membrane thickness. They gave model for evaluating optimum membrane thickness, and H_2-CO_2 separation system. For Pd membrane surface, they considered adsorption-desorption of gases. For diffusion they considered fickian diffusion. They validated model with experimental data and satisfactory results were obtained.

Meng Ni (2013) taken an autothermal reactor for supply of required heat for endothermic reaction and to provide enhanced heat transfer rate they sandwiched a thin plate of metal between catalyst layer to enhance the heat transfer rate. He investigated mass and heat transfer

within the reactor. To examine the effects of operating parameters such as gas velocity, pore size, rate of heat supply, temperature; he performed the parametric simulation. He also did comparison for different rate of heat supply.

2.3 Catalyst preparation

Shu et al., (1995) successfully tried to enhance the conversion of methane in steam reforming by developing the Pd-Ag/porous stainless steel asymmetric membranes by palladium and silver plating in electroless hydrazine baths. This was followed by hydrogen treatment of membrane above a certain temperature. This membrane was hydrogen permselective. Methane conversion was enhanced significantly by removal of produced hydrogen from upstream side. They took solution diffusion mechanism for hydrogen through Pd-membrane.

Fajardo et al., (2006) presented a simple method for preparation of catalyst of Al_2O_3 and Ni/Al_2O_3. Prepared spherical catalyst was used for hydrogen production from ethanol. They developed a method using the solution of biopolymer (chitosan) and Al. They formed a hybrid spherical compound of aluminum hydroxide and the biopolymer. In addition to their experiment they obtained spherical catalyst with large pore volume and high specific surface area through polymer elimination by thermal treatment. The Ni/Al_2O_3 spheres resulted in ethanol steam reforming, a high catalytic activity and high selectivity of hydrogen at maximum operating temperature of 650°C and best selectivity for 450°C. The plus point for catalyst formed was there was no detection of CO which indicated, for hydrogen production from ethanol, Ni/Al_2O_3 spheres a good catalyst for different industrial applications.

Houteit et al., (2006) did experiments with catalyst preparation used for hydrogen production by steam reforming of methanol. They investigated the effect of content of cesium and reaction temperature on activity of catalyst. They used the samples of copper oxide on alumina (Cu/Al_2O_3) and which was promoted with cesium ($Cu\text{-}Cs/Al_2O_3$). As compared to the undoped catalyst, the catalyst doped with cesium give higher stability and higher activity. At most favorable condition was at 300°C reaction temperature with the methanol conversion of 94 mol% and 97 mol% hydrogen selectivity for catalyst containing 2 wt % of cesium. This also showed no formation of CO. With aging treatment of catalysts, fuel conversion reached upto 100% for cesium doped catalyst.

Perez-Hernandez et. al., (2011) prepared different catalyst supports by various metal oxides in different ratios by sol-gel peptitation method. Oxides used were ZrO_2 and mixed CeO_2/ZrO_2 with the different ratios of CeO_2/ZrO_2. For the high yield of hydrogen, the support was impregnated with an aqueous solution of $NiCl_2.6H_2O$. Catalysts were characterized by BET, SEM-EDM, XRD and TPR. Using these catalysts they investigated the oxidative steam reforming of methanol for hydrogen production at various temperatures. The surface area was shown dependency on CeO_2/ZrO_2 ratio. They studied the selectivity of hydrogen as the temperature depending function.

Chen et. al., (2012) studied the performance of $YBa_2Cu_3O_{7-x}$ (YBCO) membrane with Ni/ZrO_2 as catalyst. Reactor was used for the production of hydrogen from partial oxidation of methane to syngas. The catalyst affected CO selectivity as well as methane conversion. Results

had negligible temperature effects on CO. Also the change of CH_4 leads to catalyst deactivation and decay of reactor.

De Falco (2008) simulated reformer unit and compared with traditional hydrogen reactors. Studied the effects of reactor wall temperature, gas flow rate, catalyst type and effect of residence time.

Results attested the supremacy of membrane reactors over traditional non membrane reactors. For same amount of catalyst, methane conversion reached double of non-membrane reactor conversion in magnitude. And hydrogen recovery can be enhanced by increasing the residence time therefore reactor volume. High wall temperature leads to high conversion mean time it can lead to malfunctioning of membrane, so there is a scope of optimization of wall temperature.

3. Model Development

Model use dynamic conditions within the reactor. There are two channels: Reformer and Sweep gas channel. In the first channel, catalytic steam reforming reactions take place in the presence of Ni/MgO–Al_2O_3 catalyst. Pt/δ-Al_2O_3 catalyst forms a thin layer next to the reactor wall to minimize the heat transfer resistance. Selective permeation of hydrogen through the palladium membrane is achieved in sweep gas channel. In reformer section, hot methane is fed with steam. A thin layer of palladium membrane separates reformer section from sweep gas channel. Hydrogen passes through membrane layer to reach sweep gas channel which is at lower pressure. Hydrogen in this section is swept out by nitrogen. The mixture of nitrogen and hydrogen is further processed to get pure hydrogen by gas permeation method.

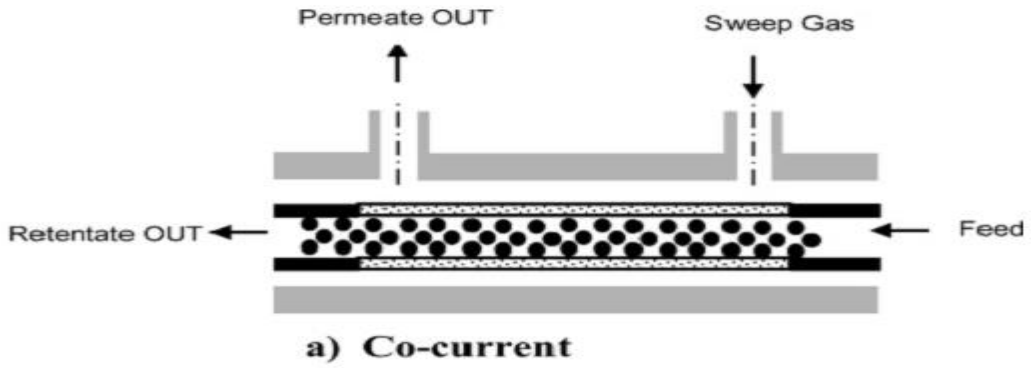

Fig: 1 illustrative diagram of the reactor

3.1. Reactions occurring in reformer:

$CH_4 + H_2O \rightarrow CO + 3H_2$, $\Delta H_{298} = 206$ kJ/mol,…….. (1)

$CO + H_2O \rightarrow CO_2 + H_2$, $\Delta H_{298} = -41$ kJ/mol,…….. (2)

$CH_4 + 2H_2O \rightarrow CO_2 + 4H_2$, $\Delta H_{298} = 165$ kJ/mol……..…….(3)

Rate equations are taken from Froment et al (1998)

$$R_1 = \frac{k_1}{P_{H2}^{2.5}}\left(P_{CH4}P_{H2O} - \frac{P_{H2}^{3}P_{CO}}{K_1}\right)\frac{1}{Q_r^{2}}$$

$$R_2 = \frac{k_2}{P_{H2}}\left(P_{CO}P_{H2O} - \frac{P_{H2}P_{CO2}}{K_2}\right)\frac{1}{Q_r^{2}}$$

$$R_3 = \frac{k_3}{P_{H2}^{3.5}}\left(P_{CH4}P_{H2O}^{2} - \frac{P_{H2}^{4}P_{CO2}}{K_3}\right)\frac{1}{Q_r^{2}}$$

where,

$$Q_r = (1 + K_{CO}P_{CO} + K_{H2}P_{H2} + K_{H2O}P_{H2O} + (K_{CH4}P_{CH4})/P_{H2})$$

3.2. Model assumptions

In this study, the plate-plate geometry is considered for the reactor. Reactor is divided into two sections: Reformer section and Sweep gas section. Both the sections are separated by a thin leyer of palladium membrane. Only Hydrogen out of all reaction products passes through membrane to the sweep gas channel. In

sweep gas channel hydrogen is swept out by use of nitrogen, an inert gas. The steam reformer is modeled as the pseudo-homogenous reactor.

The basic model assumptions are:

(1) Plug flow behavior of gas mixture is assumed in the reformer, with negligible radial gradients of concentrations and temperature.

(2) Pseudo-homogenous model of the reformer.

(3) Constant bed porosity in axial and radial directions.

(4) Ideal membrane behavior with infinite selectivity for hydrogen.

(5) Non-adiabatic reactor

(6) Non-isothermal reactor

(7) Reformer gases and sweep gases are ideal gases.

3.3. Component indexes of gas species in the reactor

Component species	Index (reformer)	Index (Sweep gas)
Methane	1	Not applicable
Steam	2	Not applicable
Hydrogen	3	1
Carbon dioxide	4	Not applicable
Carbon monoxide	5	Not applicable
Nitrogen	Not applicable	2

3.4 Hydrogen permeation

Hydrogen permeation rate through membrane is represented by a power-law expression.

$$J = \frac{Q_0 \exp(-E_p/RT)}{\tau}\left(\sqrt{p_{r,H2}} - \sqrt{p_{m,H2}}\right)$$

The membrane is assumed to perform ideally which only allow permeation of hydrogen. The values of the pre-exponential factor (Q_0) and the activation energy (E_P) are taken as 6.33×10^{-7} mol/(mPa$^{1/2}$ s) and 15,700 J/mol, respectively.

3.5 Mass Balances Equations:

3.5.1 Reformer:

Mass balance equations for all components in the reformer except hydrogen are:

[Mass velocity of component species input] – [mass velocity of component species output] + [mass rate of generation of component species] = [mass rate of transport trough membrane] + [Rate of accumulation of component species]

$$\varepsilon \frac{\partial}{\partial t} C_{r,i} + \varepsilon \frac{\partial}{\partial z} (u_r C_{r,i}) + J_i S_m (t_m / t_r) = \rho_r r_{r,i}$$

$$\varepsilon \frac{\partial}{\partial t} C_{r,i} + \varepsilon \frac{\partial}{\partial z} (u_r C_{r,i}) = \rho_r r_{r,i}$$

3.5.2 Sweep gas channel:

$$\frac{\partial}{\partial t} C_{m,i} + \frac{\partial}{\partial z} (u_m C_{m,i}) = J_i S_m$$

$$\frac{\partial}{\partial t} C_{m,i} + \frac{\partial}{\partial z} (u_m C_{m,i}) = 0$$

3.6 Energy Balances Equations:

3.6.1 Reformer:

[Heat consumed due to reformer reactions] + [Convective heat transfer from wall to reformer] + [Energy transport associated with hydrogen permeation] + [Convective heat transfer from membrane to reformer] = [Energy accumulation within reformer]

$$\frac{\partial}{\partial t}(\rho_r Cp_r T_r) + \frac{\partial}{\partial z}(u_r \rho_r Cp_r T_r) - \rho_r \sum_j R_j(-\Delta H_j) - \frac{h_{r,w}}{t_r}(T_w - T_r) -$$

$$S_m \left(\frac{t_m}{t_r}\right)(1 - \delta_{H2}) J\left(H_{r,H2} - H_{m,H2}\right) - \frac{h_{r,m}}{t_r}(T_m - T_r) = 0$$

3.6.2. Sweep gas channel

[Heat accumulated in membrane] =

[Convective heat transfer from reformer to membrane] + [Heat flow by hydrogen permeation]

$$\frac{\partial}{\partial t}\left(\rho_m c_{p,m} T_m\right) + \frac{\partial}{\partial z}\left(u_m \rho_m c_{p,m} T_m\right) - \frac{h_{r,m}}{t_r}(T_m - T_r)$$

$$- S_m(1 - \delta_{H2}) J\left(H_{r,H2} - H_{m,H2}\right) = 0$$

3.7. Momentum Balance equation

$$\frac{1}{u_r}\frac{\partial P_r}{\partial t}+\frac{\partial P_r}{\partial z}+u_r\rho_r\frac{\partial u_r}{\partial x}=-f$$

$$f=150\frac{(1-\varepsilon)^2}{\varepsilon {d_p}^2}u_r\mu_r+1.75\frac{(1-\varepsilon)\rho_r {u_r}^2}{\varepsilon d_p}$$

To complete balance, relationship of concentration to total pressure is given

$$P_r=R_gT_r\sum_{i=1}^{5}C_{r,i}$$

$$P_m=R_gT_m\sum_{i=1}^{2}C_{m,i}$$

3.8. Boundary conditions

In this section the set of boundary conditions have been given and discussed, to solve the model equations. The known terminal compositions, temperatures and pressure are used for each corresponding component in each section. Sections consider here are reformer section and sweep gas channel. The index is for different components in corresponding section. In reformer i is for methane, steam, carbon monoxide, hydrogen, and carbon dioxide. In sweep gas channel, i is for nitrogen and hydrogen only. All compositions are known at entrance of reactor and at the exit of reactor. At the entrance of the reactor, the inlet temperatures and the inlet gas compositions of the reformer gas and the sweep gas are known. Therefore, the following boundary conditions are applicable at z = 0:

I. At time less than zero, there is no reaction taking place in the reactor so the values considered here, for t< 0, initial values.

$t < 0$

$C_{r,i} = C_{r,i}(0), \quad \forall\ i$

$T_{r,i} = T_{r,i}(0), \quad \forall\ i$

$P_{r,i} = P_{r,i}(0), \quad \forall\ i$

$C_{m,i} = C_{m,i}(0), \quad \forall\ i$

$P_{m,i} = P_{m,i}(0), \quad \forall\ i$

II. Since the diffusional mass transfer is zero axially at both the terminals of reactor catalyst layer, "Danckwert's boundary conditions" is applicable here to relate the concentrations in reactor. Similarly, the conductive heat transfer is zero in axial direction at both terminals of reactor. Thus the boundary condition for temperature, temperature gradient is zero for time greater than zero at reactor terminals i.e. for z is zero and at other end of reactor i.e. when z is L. Therefore, the under mentioned boundary conditions are applicable at both terminals of the reactor

$t \geq 0$, for both reformer and sweep gas channel, BCs are:

at $C_i(0,t)$ and $C_i(L,t)$; $\partial C_i/\partial z = 0\ \forall$ i

at $T_i(0,t)$ and $T_i(L,t)$; $\partial T_i/\partial z = 0\ \forall$ i

at $P_i(0,t)$ and $P_i(L,t)$; $\partial P_i/\partial z = 0\ \forall$ i

3.9. Heat and mass transfer coefficients:

- Heat transfer coefficient of reformer wall can be estimated using the relationship given by Froment GF.

$$h_{r,w} = 0.813\left(\frac{\lambda_r}{d_r}\right)\exp\left(\frac{-6d_p}{d_r}\right)\left(\frac{d_p u_r \rho_r}{\mu_r}\right)^{0.9}$$

- Same for reformer and sweep gas, $h_{m,w}$ is 2.4 W/m^2K.
- Enthalpy of the components in the reformer section is modeled as

$$H_i = \int_{T_{ref}}^{T} c_{p,i}\, dT$$

Where "heat capacity of gas species" is calculated as a temperature function

$$C_{p,i} = a_i + b_i T + c_i T^2 + d_i T^3$$

3.10. Table 3.2 Coefficient for specific heat expressions:

Gas	**A**	**b*10^2**	**c*10^5**	**d*10^9**
CO_2	36.11	4.233	-2.887	7.464
CO	28.95	0.411	0.3548	-2.22
H_2	28.84	0.00765	0.3288	-0.8698
N_2	29	0.2199	0.5723	-2.871
CH_4	34.31	5.469	0.3661	-11
H_2O	18.2964	47.212	-133.88	1314.2

Viscosity of the reformer gas mixture is evaluated as a function of concentration and temperature using the Lucas corresponding states methods. Binary diffusion coefficient is given by the empirical correlation by Fuller et al.

$$D_{ij} = \frac{0.01013 T_b^{1.75} [(M_i + M_j)/M_i M_j]^{1/2}}{P_b [(\sum \upsilon)_i^{1/3} + (\sum \upsilon)_j^{1/3}]^2}$$

From the binary diffusion coefficient, the diffusion coefficient for multi-component gas mixture can be modeled using the following relation

$$D_{mix,i} = \frac{1 - y_i}{\sum_j (y_i / D_{ij})}, j \neq i$$

The effective diffusion coefficient in the catalyst layer is calculated using the following relation

$$\mathrm{D_{eff,i}} = \frac{\varepsilon}{\tau}\left(\frac{1}{\mathrm{D_{k,i}}} + \frac{1}{\mathrm{D_{mix,i}}}\right)^{-1}$$

Where, Knudsen diffusion coefficient, $D_{K,i}$ can be calculated from the correlation proposed by Hayes and Kolaczkowski

$$\mathrm{D_{k,i}} = \frac{\mathrm{d_p}}{3}\left(\frac{8\,\mathrm{RT}}{\pi \mathrm{M_i}}\right)$$

Thermal conductivity of the reactor wall can be found from

$$\lambda_w = 10.738+0.0242T_w$$

From the component thermal conductivities, the mixture thermal conductivity can be estimated using the method of Lindsay and Bromley.

Thermal conductivity of mixture is estimated by Bromley and Lindsay method which compute the conductivity of mixture by that of individual components.

Table 3.3 Design specifications and operating variables for the reference case

Design specification/operating variable	Value
Reactor length	1.2 m
Reformer channel thickness	0.01m
Sweep gas channel thickness	0.02m
Wall thickness	0.001m
Membrane thickness	$4.5x10^{-6}$ m
Reformer catalyst density	2270 kg/m^3
Reformer catalyst particle size	0.00018m
Reformer bed void fraction	0.33
Reformer pressure	5 bar
Sweep gas pressure	1 bar
Steam/methane ratio	3
Reformer inlet gas temperature	765 K
Sweep gas inlet temperature	400K
Reformer inlet gas velocity	0.8 m/s
Sweep gas inlet velocity	3 m/s
Flow mode	Cocurrent

4. Modus operandi to Solve the Model

- The formulated model having of 13 partial differential equations (equation 8 to 20) including 2 second order partial differential equations (16 & 18) and the associated boundary conditions (21 & 22) lends itself to be a boundary value problem. The partial differential model equations are first discretized using forward difference method.
- The reactor length (1.2m) is divided into 10 intervals with two collocation points in each interval. So the total no of points become 31 which means every differential convert in 37 algebraic equations. These 403 (31 points *13 variables) equations along with other algebraic equations are to be solved simultaneously
- Apart from discretized algebraic equations in the model there are the boundary conditions, the reaction rates, the ideal gas assumption, Ergun's relation for the pressure drop, as well as the correlations for the heat and mass transfer coefficients and the properties for the fluid, catalyst and the reactor wall and hydrogen permeation rate. These equations along with the discretized differential equations form a set of nonlinear algebraic equations.
- This set of equations is to be solved using code written in C++.

5. Results and Discussions

The performance of membrane reactor is analyzed, using different operating variables, for methane conversion and hydrogen recovery yield

$$\text{Methane conversion (\%)} = \frac{F_{CH_4,in} - F_{CH_4,out}}{F_{CH_4,in}} X100$$

The hydrogen recovery yield is defined as follows

$$\text{Hydrogen recovery yield} = \frac{F_{m,H_2}}{F_{CH_4,in}}$$

As expected, it can be observed from the fig 5.1 that concentration of reactants (CH_4 and H_2O) decreases while that of products (CO, CO_2, H_2) increases with bed length. The concentration of CO can be observed to be very low throughout the bed length. This is due to the shift reaction taking place in which the CO produced gets converted into CO_2 leading to a rise in CO_2 concentration at the same time. From the graph, it can be seen that about 95% of reactant conversion takes place at about 0.7 m bed length. Thus, reaction being endothermic, the concentration of reactants and products reaches a steady state value due to very low availability of reactants after bed length of 0.7m.

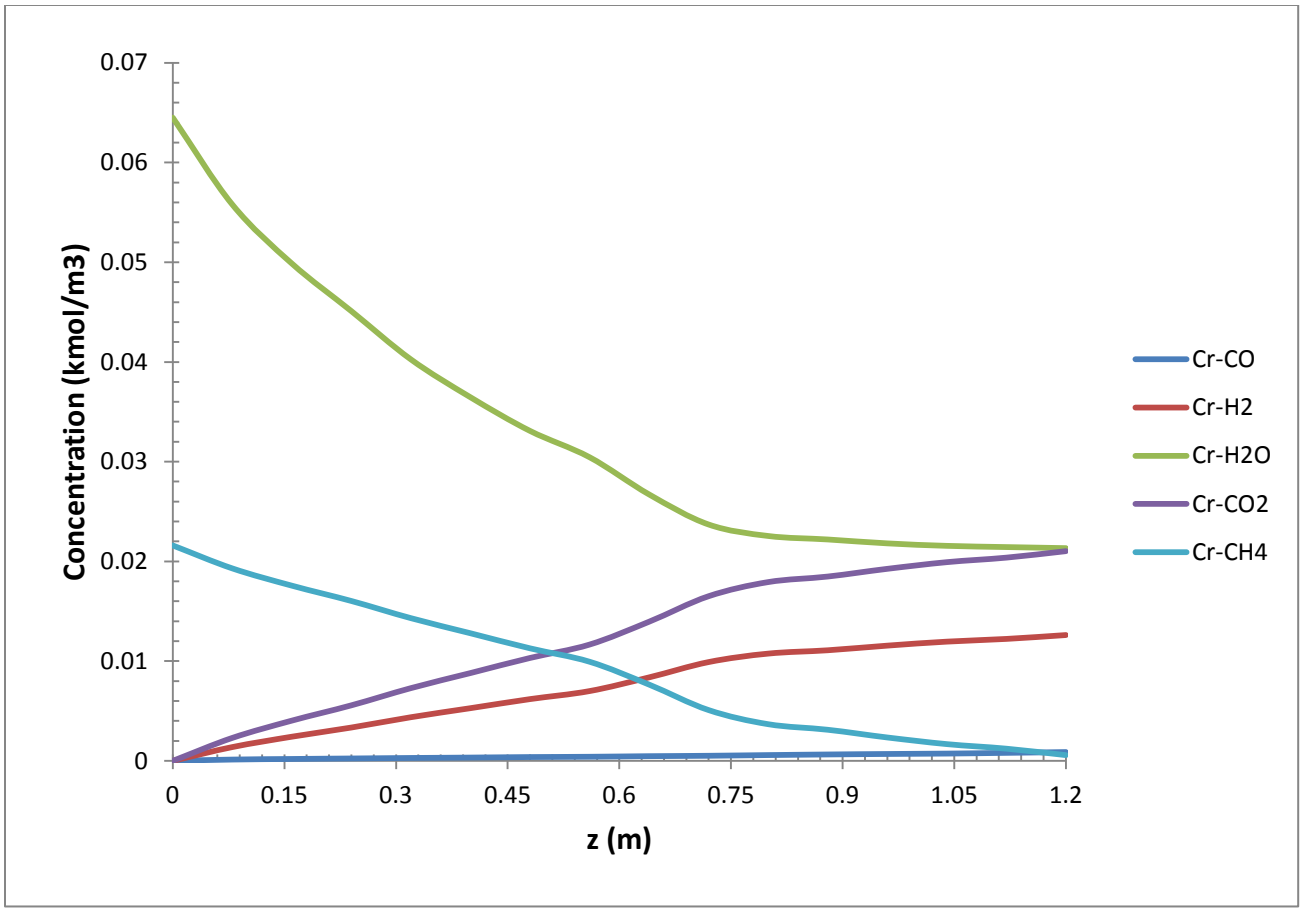

Figure 5.1 Concentration profile for reformer gas along the reformer bed

Fig 5.2 shows the temperature profiles of reformer wall (T_w), reformer (T_r), membrane (T_m) and sweep gas channel. All the temperature profiles except that of reformer temperature show an increasing trend.

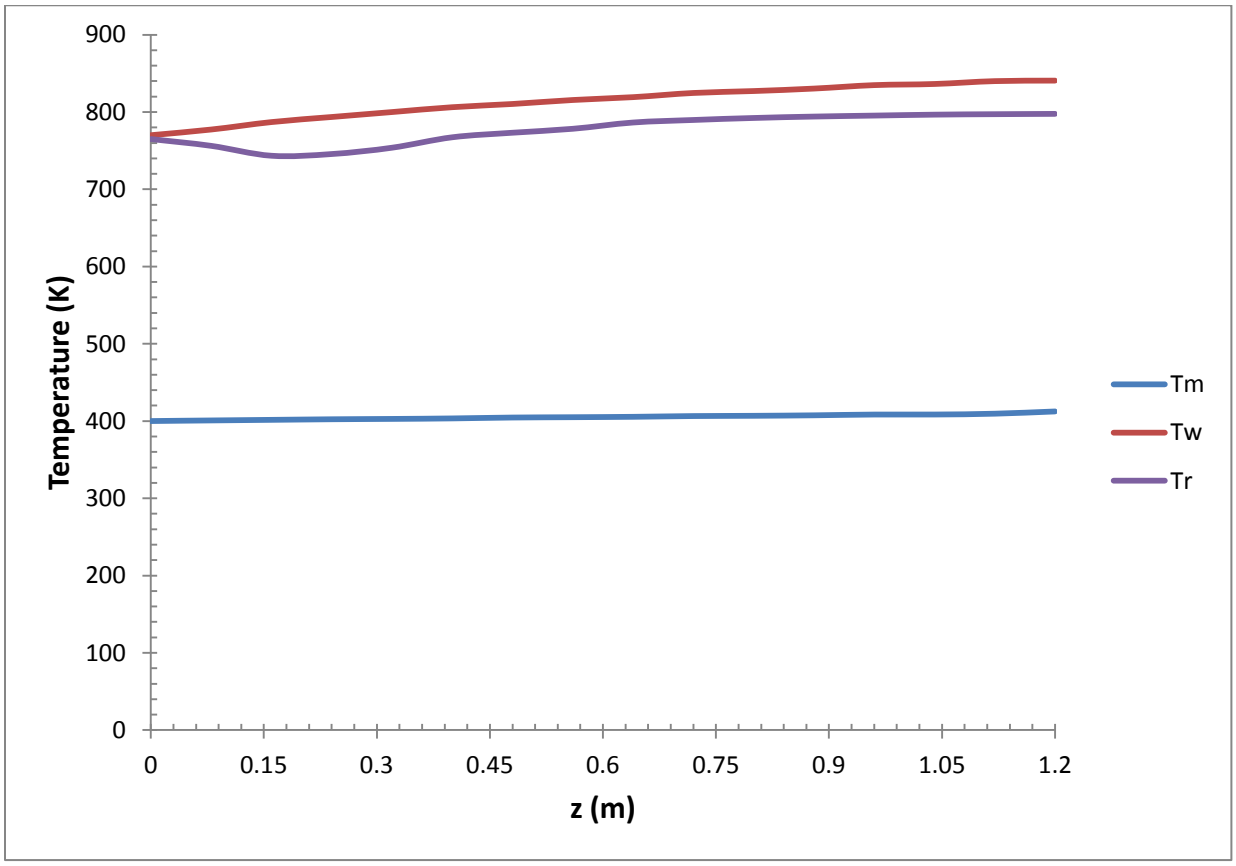

Figure 5.2 Temperature profiles

It's interesting to note the form of Reformer temperature profile. There is a decrease in temperature in the initial part (i.e. near the inlet of the bed). This is due to the fact that the rate of reforming reaction is higher around this region due to high concentration of reactants available and reaches to the value 797 K. The variation of reformer pressure along the reactor length is shown in fig 5.3. Due to small particle size considerable pressure drop is observed which limits the inlet velocity of the reformer gas.

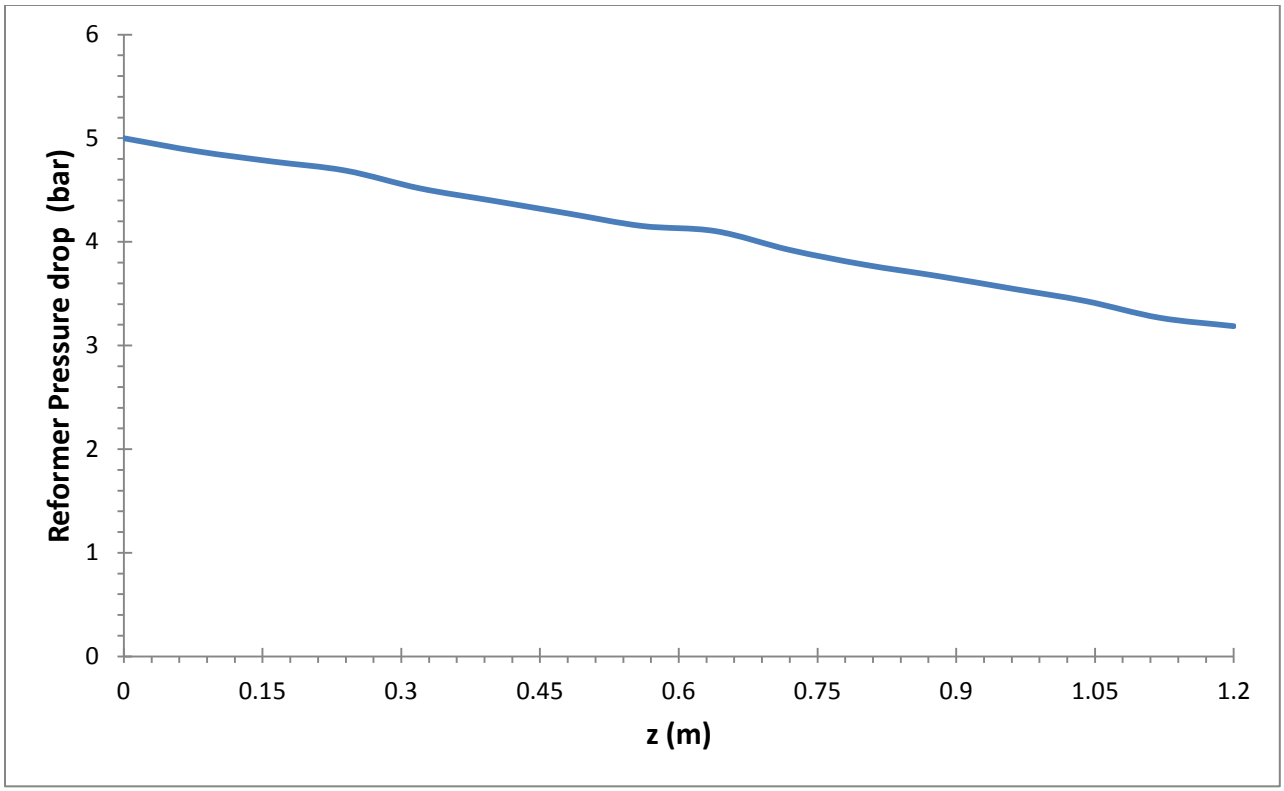

Figure 5.3 Pressure drop profile in reformer

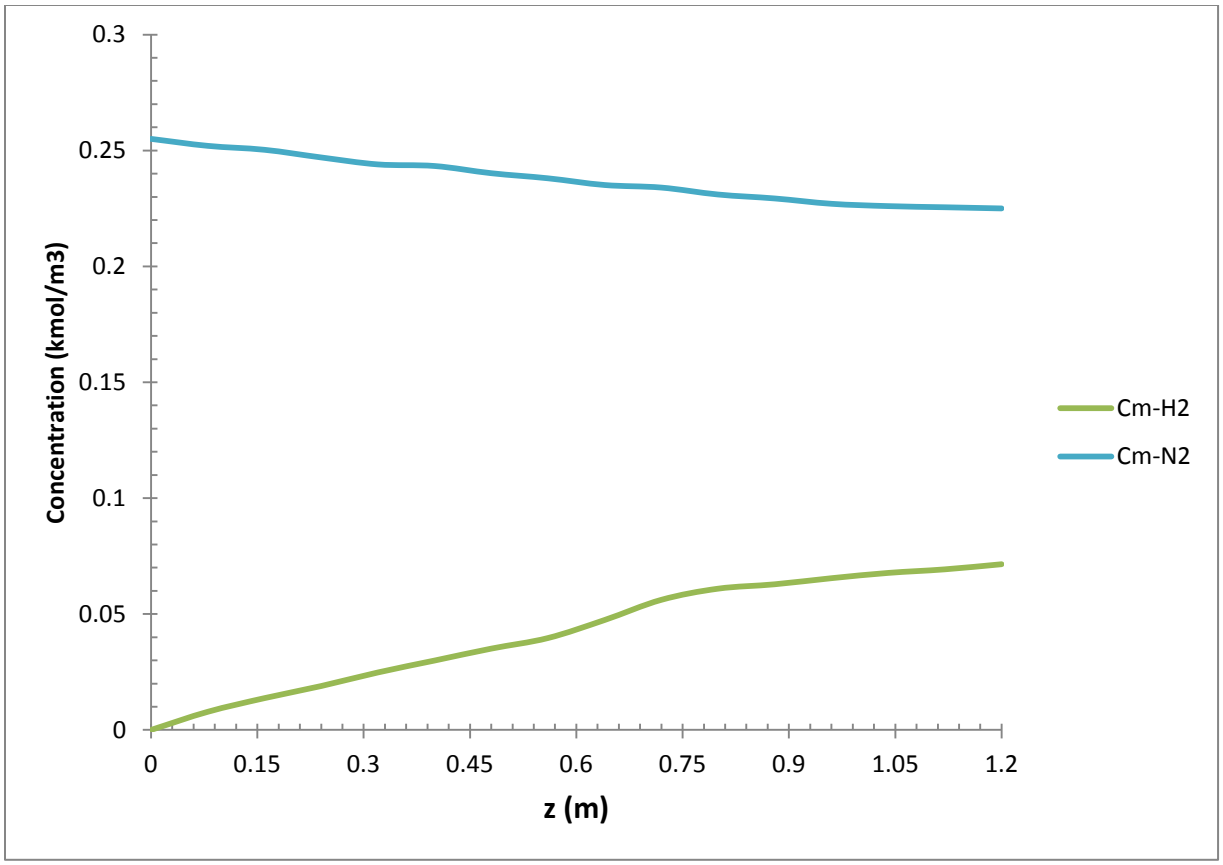

Figure 5.4 Concentration profile of N_2 and H_2 in membrane reactor

Fig 5.4 demonstrates the concentration profiles of N_2 and H_2 in membrane reactor. Here, N_2 is being used as a `sweep gas' to sweep H_2 out of the membrane. It can be observed that as we move along the bed length, the H_2 concentration increases as the hydrogen produced is getting separated through the membrane. At the same time, N_2 concentration goes on decreasing due to an increase in total volume of the gas mixture with reaction coordinates.

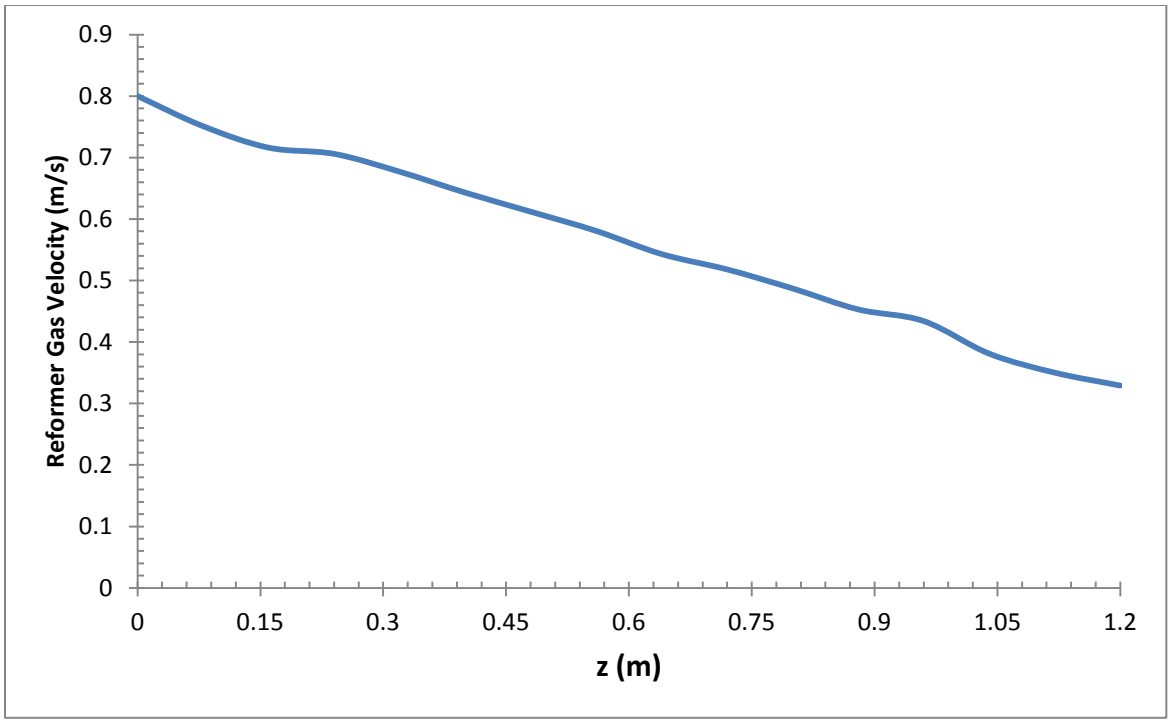

Figure 5.5 Reformer gas velocity

A general decrease in the values of reformer gas velocity is observed in fig 5.5 as we travel along the bed length. This can be attributed to the fact that H_2 is being removed from the reaction mixture through a membrane. Also, velocity decreases due to pressure drop in the reformer bed due to gas flow.

5.1 Effect of introduction of membrane of different types:

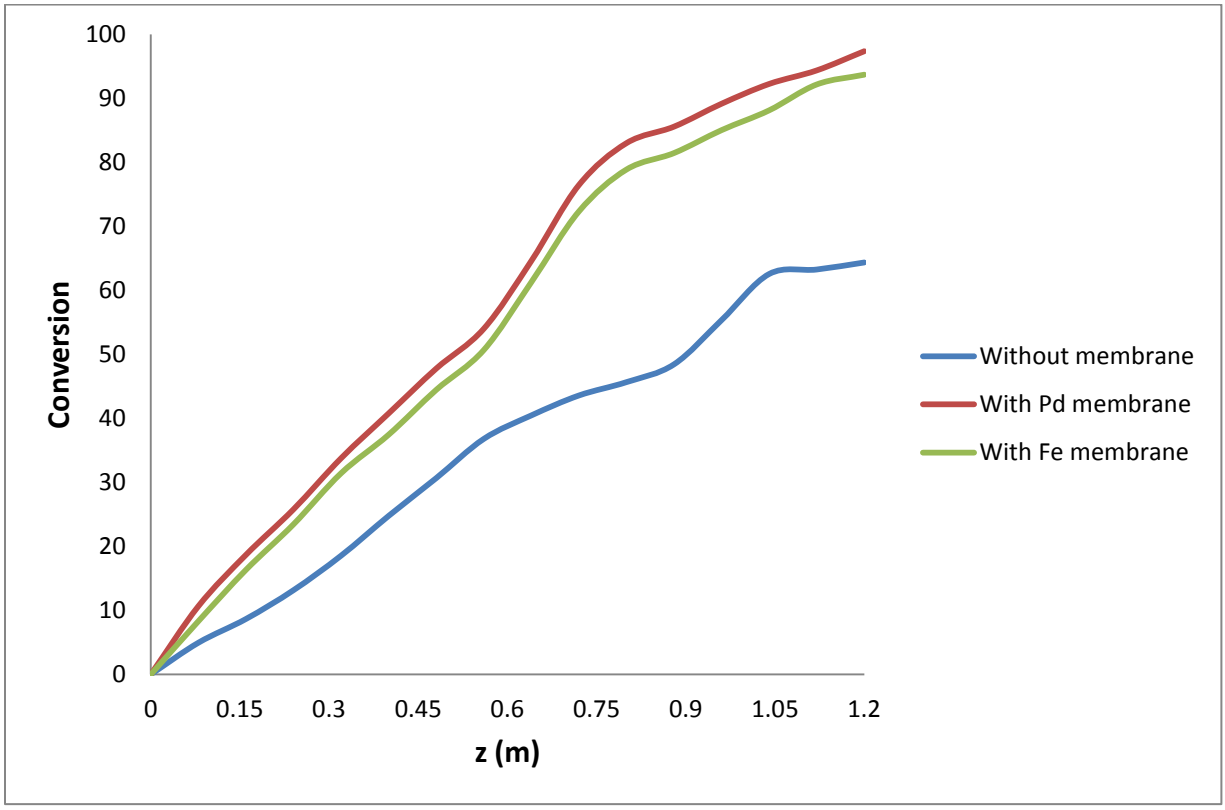

Figure 5.6 Conversion profile for methane with and without membrane

The mechanism for H_2 separation by a metal membrane is often referred to as the ‘‘solution-diffusion’’ mechanism. Hydrogen is transported through the metal membrane in a series of steps that include the adsorption of H_2 onto the surface, its dissociation into ions and electrons, its absorption or dissolution into the metal, its diffusion through the bulk of the metal, its re-association on the metal surface before desorption as a gas. The metal structure is sufficiently dense that it greatly restricts the ability of other gas molecules to diffuse through the metal, thereby separating the H_2.

The trends in the fig 5.6 and fig 5.7 show the conversion and hydrogen recovery yield respectively of methane reforming reaction, with 2 different types of membranes as well as without any membrane. The membrane performs the function of selectively separating the hydrogen from reactant-product mixture in reformer. At any point along the bed length, it is clear that the conversion and hydrogen recovery yield in the case where membrane is there (both Fe and Pd), conversion and yield are considerably higher as compared to the case where no membrane is present (64.34% / 1.429). It can also be seen that Pd offers a better permeation of hydrogen as compared to Fe which reflected in higher conversion and yield values for Pd membrane (97.34% / 3.89) than Fe membrane (93.6% / 3.49). The reason for higher conversion and yield when membrane is present is that it removes the product hydrogen from the reaction mixture thus enhancing the forward rate of reaction.

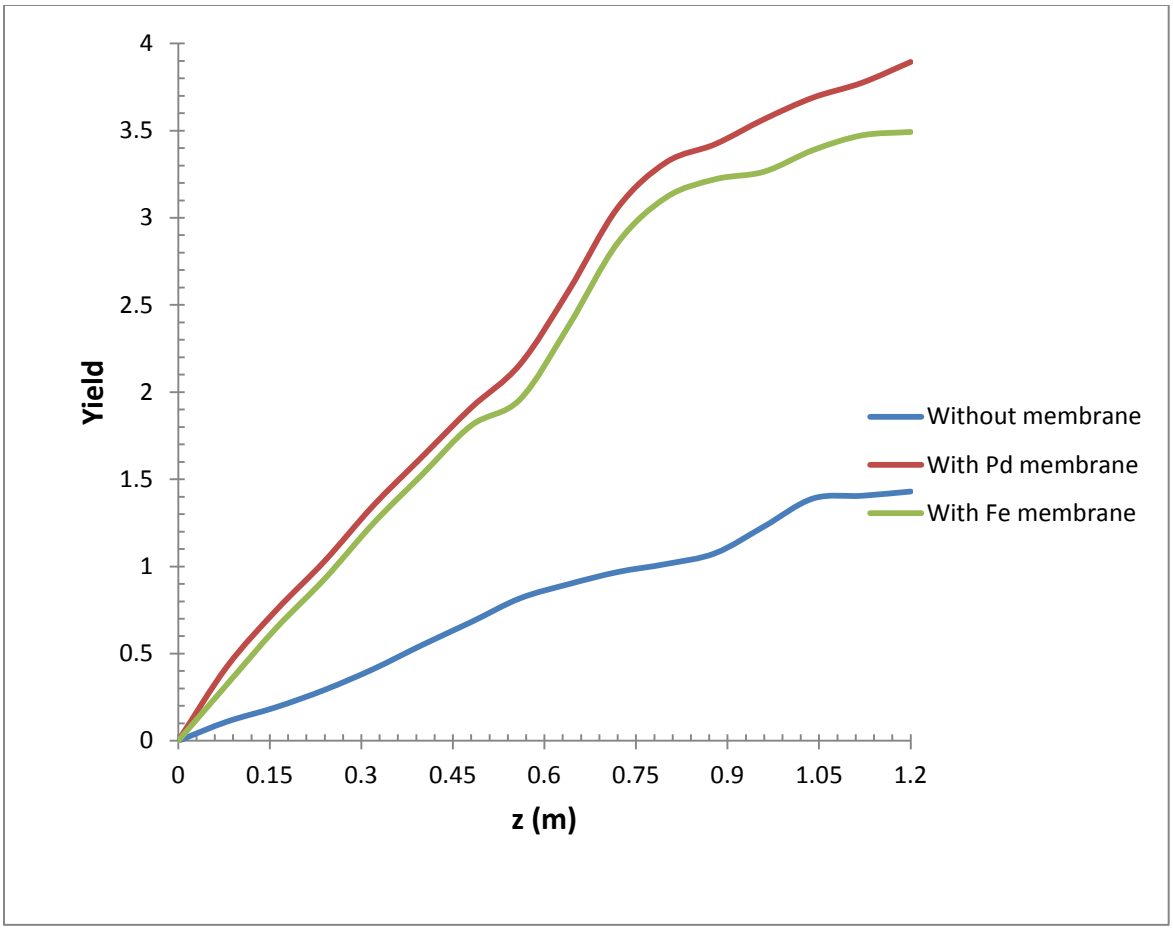

Figure 5.7 Hydrogen recovery yield

When we compare the hydrogen permeability and ΔH formation of hydrides data for Pd and Fe membranes, we find out that the permeability is significantly higher for Pd ($1.9x10^{-8}$) as compared to Fe ($1.8x10^{-10}$) also; the ΔH is +20 (Pd_2-H) kJ/mol and +14 (Fe-H) kJ/mol. Thus, it is clear that Pd is a better membrane for H_2 separation, hence leading to higher conversion and yield.

5.2 Effect of Steam/methane ratio on methane conversion and yield

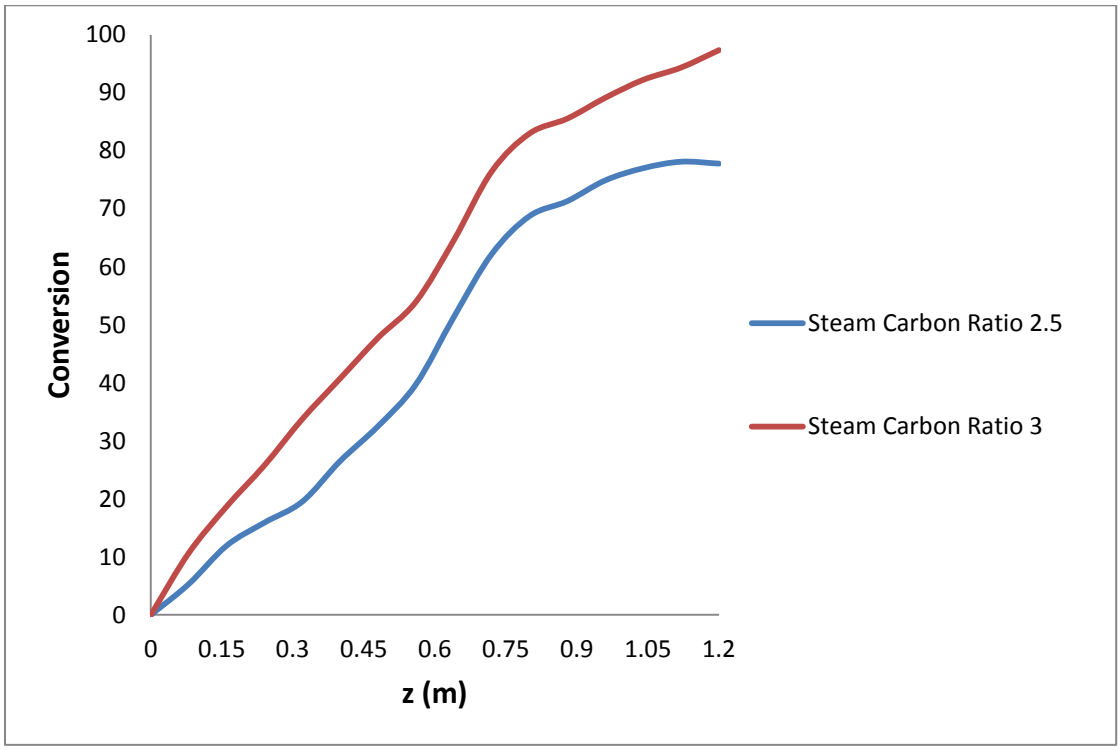

Figure 5-8 Conversion with steam to methane ratio

It is always desirable to have a higher steam carbon ratio for a higher conversion of methane in steam reforming. If the steam to methane ratio increases the energy requirement for reforming reaction reduced due to reduced flow rate of methane. As a results of it methane conversion and yield increase with increase in steam to methane ratio. It can also be explained in fig 5.8 and fig 5.9 as a higher ratio means higher probability of effective collisions between reactants leading to product formation. Plots show that the conversion and yield are higher (97.34% / 3.89) when steam carbon ratio is 3 as compared to when the ratio is 2.5(77.78% / 3.11). A higher steam ratio is also beneficial from the point of view of carbon deposition on catalyst as it lessens the same. At the same time, we cannot increase the ratio to a very high value owing to economic constraints.

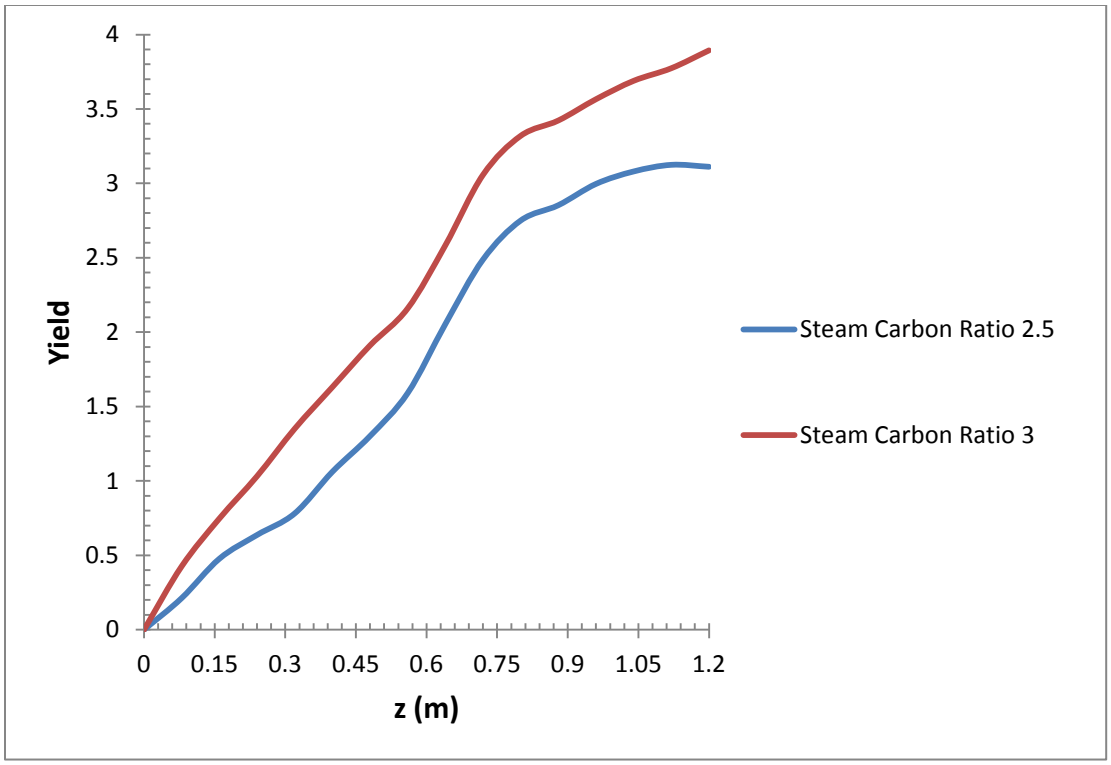

Figure 5-9 Yield with steam to methane ratio

5.3 Effect of inlet gas temperature on methane conversion and hydrogen recovery yield

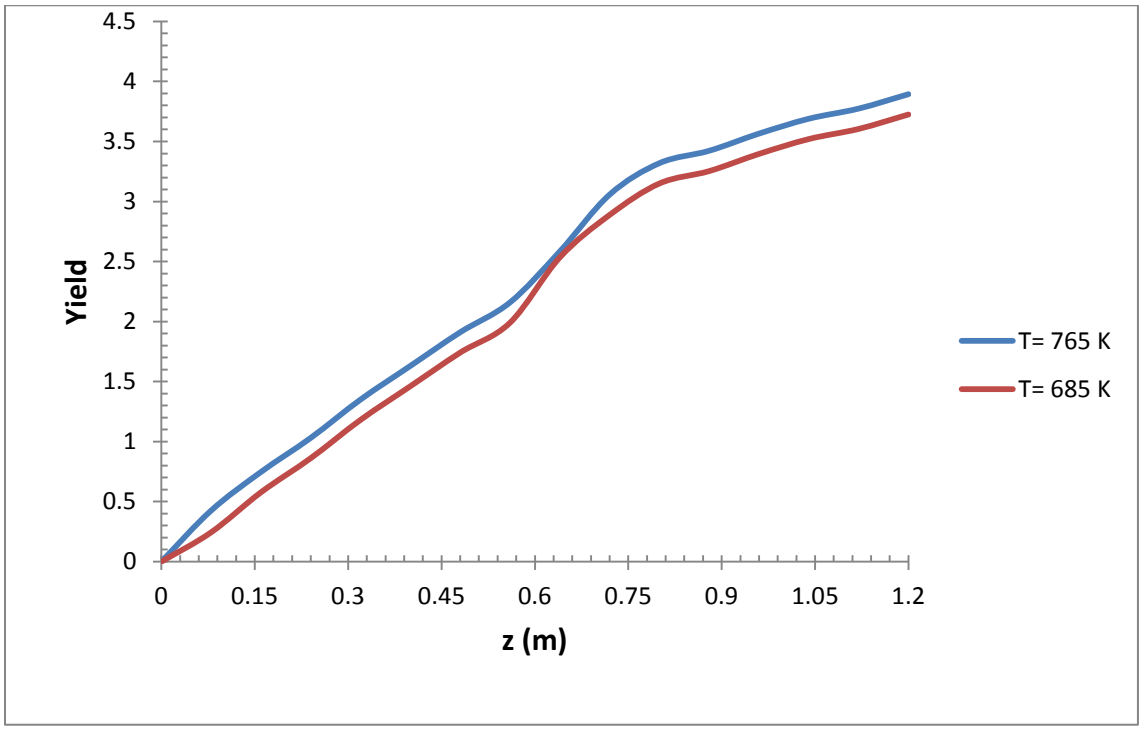

Figure 5.10 Hydrogen recovery yield with inlet gas temperature

The reformer reaction is endothermic in nature. Thus it is clear from Le-Chataliers principle that if we increase the inlet temperature, it will have a positive impact of the overall conversion and yield of the reaction. The same result can be observed in fig 5.10 and fig 5.11. At any point along the bed length, conversion and yield when T_{in}=765K is higher (97.34% / 3.89) as compared that when T=685K (93.11% / 3.72).

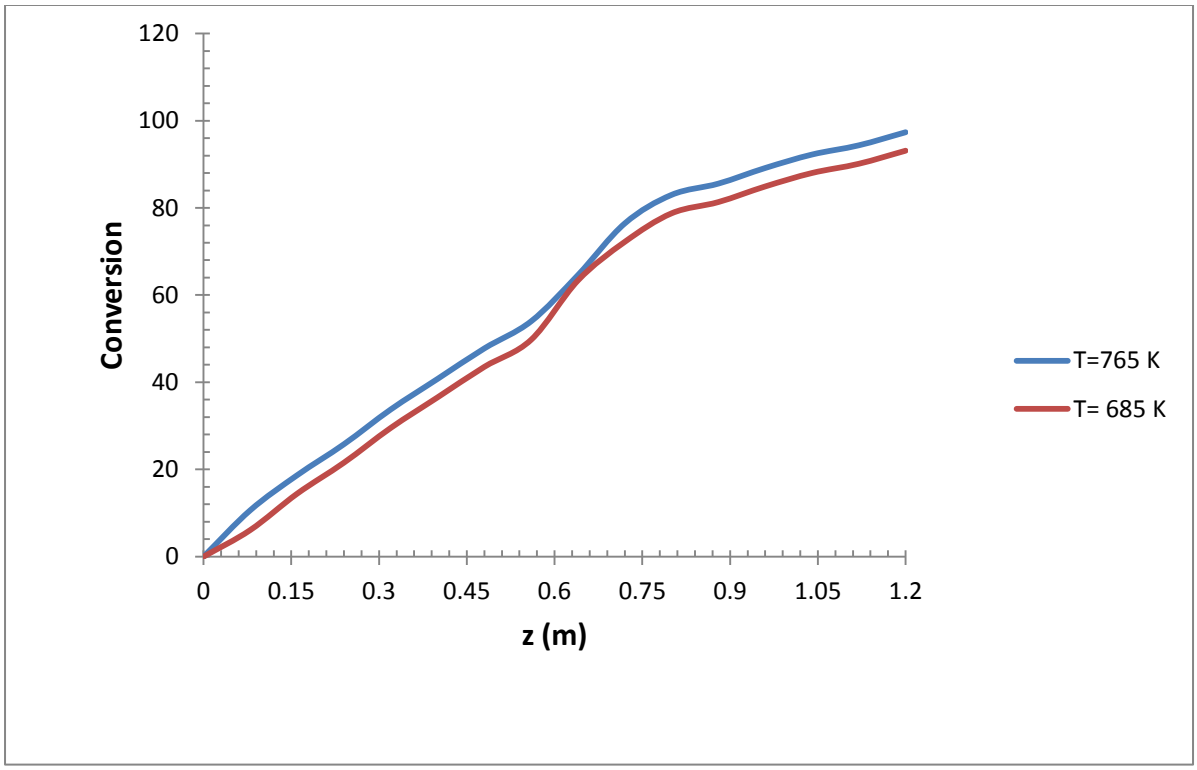

Figure 5.11 Conversion with inlet gas temperature

5.4 Effect of reformer inlet velocity on methane conversion and hydrogen recovery yield

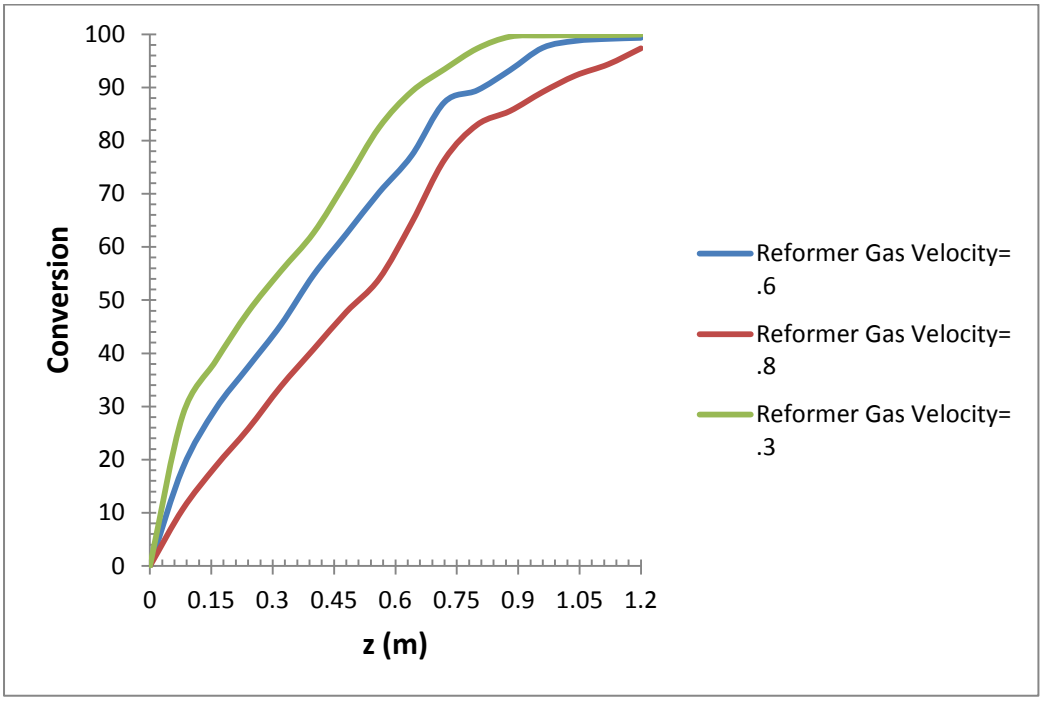

Figure 5.12 Conversion with reformer inlet velocity

The profile of methane conversion and hydrogen recovery yield for different reformer inlet velocities are shown in fig 5.12 and fig 5.13. As shown in the figure if the reformer inlet velocity is 0.3 m/s, methane conversion and hydrogen recovery yield reach their maximum value by just 0.8 m of reactor length. This is due to the high residence time and the low energy requirement for the reforming reaction at low reformer inlet velocities. If the reformer inlet velocity increases to 0.6 m/s, 1.04 m of reactor length is utilized. With further increase in reformer inlet velocity to 0.8 m/s the conversion and yield increases along the whole length of reactor.

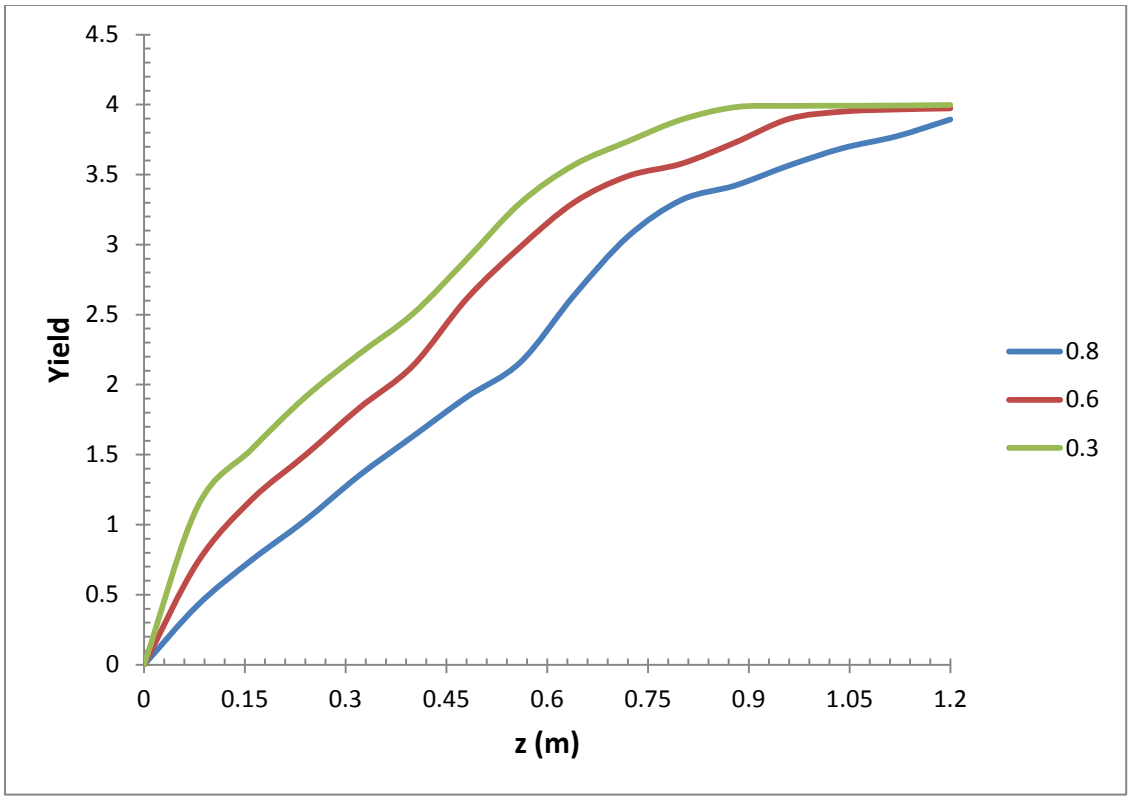

Figure 5.13 Yield with reformer inlet velocity

- **Crank Nicolson Method**

- $\epsilon\frac{{C_{ri}}^{a+1,b}-{C_{ri}}^{a,b}}{\Delta t}+\epsilon\frac{{u_r}^{a,b}}{2(\Delta z)}\left({C_{ri}}^{a+1,b+1}-{C_{ri}}^{a+1,b-1}+{C_{ri}}^{a,b+1}-{C_{ri}}^{a,b-1}\right)+\epsilon\frac{{C_{ri}}^{a,b}}{2(\Delta z)}\left({u_r}^{a+1,b+1}-{u_r}^{a+1,b-1}+{u_r}^{a,b+1}-{u_r}^{a,b-1}\right)=\rho_r r_{ri}-J_i S_m\left(\frac{t_m}{t_r}\right)$

- $\frac{{C_i}^{a+1,b}-{C_{mi}}^{a,b}}{\Delta t}+\frac{{u_m}^{a,b}}{4(\Delta z)}\left({C_{mi}}^{a+1,b+1}-{C_{mi}}^{a+1,b-1}+{C_{mi}}^{a,b+1}-{C_{mi}}^{a,b-1}\right)+\frac{{C_{mi}}^{a,b}}{2(\Delta z)}\left({u_{mi}}^{a+1,b+1}-{u_{mi}}^{a+1,b-1}+{u_{mi}}^{a,b+1}-{u_{mi}}^{a,b-1}\right)=J_i S_m$

- $\frac{h_{sw}}{t_w}(T_s-T_w)+\frac{h_{rw}}{t_w}(T_r-T_w)=-\frac{\lambda_w}{2\Delta x^2}[(T_r^{j+1,i+1}-2T_r^{j+1,i}+T_r^{j+1,i-1})+(T_w^{j,i+1}-2T^{j,i}+T^{j,i-1})]$

- ${\rho_r}^{a,b}c_{pr}\left(\frac{{T_r}^{a+1,b}-{T_r}^{a,b}}{\Delta t}\right)+{\rho_r}^{a,b}{T_r}^{a,b}\left(\frac{{c_p}^{a+1,b}-{c_p}^{a,b}}{\Delta t}\right)+c_{pr}{T_r}^{a,b}\left(\frac{{\rho_r}^{a+1,b}-{\rho_r}^{a,b}}{\Delta t}\right)+\frac{u_r c_{pr}\rho_r}{4.\Delta z}\left({T_r}^{a+1,b+1}+{T_r}^{a+1,b-1}+{T_r}^{a,b+1}+{T_r}^{a,b-1}\right)+\frac{u_r c_{pr}T_r}{4.\Delta z}\left(\left({\rho_r}^{a+1,b+1}+{\rho_r}^{a+1,b-1}+{\rho_r}^{a,b+1}+{\rho_r}^{a,b-1}\right)\right)+\frac{u_r T_r\rho_r}{4.\Delta z}\left({c_{pr}}^{a+1,b+1}+{c_{pr}}^{a+1,b-1}+{c_{pr}}^{a,b+1}+{c_{pr}}^{a,b-1}\right)+\frac{T_r c_{pr}\rho_r}{4.\Delta z}\left({u_r}^{a+1,b+1}+{u_r}^{a+1,b-1}+{u_r}^{a,b+1}+{u_r}^{a,b-1}\right)={\rho_r}^{a,b}\sum_j {R_j}^{a,b}\left(-\Delta {H_j}^{a,b}\right)+\frac{h_{rw}}{t_r}\left({T_w}^{a,b}-{T_r}^{a,b}\right)+\frac{h_{rm}}{t_r}\left({T_m}^{a,b}-{T_r}^{a,b}\right)+S_m(t_m/t_r(1-\delta_{H2})\,{J_i}^{a,b}$

6. References

1. Arpornwichanop, A., Wasuleewan, M., Patcharavorachot, Y., Assabumrungrat, S. "Investigation of a Dual-Bed Autothermal Reforming of Methane for Hydrogen Production" *Chemical Engineering Transactions* **25**, pp. 929-934,2011.
2. Barbieri G. Francesco P. "Simulation of the methane steam re-forming process in a catalytic pd-membrane reactor". *Ind. Eng. Chem. Res.*, 1997, **36 (6)**, pp 2121–2127".
3. "Boor CD. A practical guide to splines. New York: Springer; 1978".
4. "Cengel YA, Turner RH. Fundamentals of thermal fluid science. New York: McGraw-Hill; 2001".
5. Chen Z, Prasad P, Yan Y, Elnashaie S. "Simulation for steam reforming of natural gas with oxygen input in a novel membrane reformer". *Fuel Process Technology* 2003; **83**:235–52.
6. De Falco, M., "Pd-based membrane steam reformers: A simulation study of reactor performance", 2008; *Hydrogen Energy*, **33**, 3036-40.
7. "Ergun S. "Fluid flow through packed columns". *Chem Eng Prog* 1952;48: 89–94".
8. Frauhammer J, Eigenberger G, Hippel LV, Arntz D. "A new reactor concept for endothermic high-temperature reactions". *Chem Engg Sci* 1999; **54**:3661–70.
9. Froment GF. Chemical reactor analysis and design. New York: Wiley; 1990".
10. Fuller EN, Schettler PD, Giddings JC. "New method for prediction of binary gas phase diffusion coefficients". *Ind Eng Chem* 1966; **58(5)**:18.
11. Furimsky E. "Selection of catalysts and reactors for hydroprocessing". *Applied Catalyst-A* 1998; **171**:177–206.
12. Gallucci F, Paturzo L, Basile A. "A simulation study of the steam reforming of methane in a dense tubular membrane reactor". International Journal of Hydrogen Energy 2004; **29**:611–7.
13. Giuseppe B, Francesco PDM. "Simulation of the methane steam reforming process in a catalytic Pd-membrane reactor". *Ind Engg Chem Res* 1997; **36**:2121–7.
14. Hoang DL, Chan DL. "Modeling of a catalytic autothermal methane reformer for fuel cell applications". *Applied Catalyst-A* 2004; **268**:207–16.
15. Incropera FP, DeWitt DP. "Introduction to heat transfer". New York: Wiley; 1990.

16. Lattner JR, Harold MP. "Comparison of conventional and membrane reactor fuel processors for hydrocarbon-based PEM fuel cell systems". *Int J Hydrogen Energy* 2004; 29:393–417.
17. "Lin YM, Liu SL, Chuang CH. "Effect of incipient removal of hydrogen through palladium membrane on the conversion of methane steam reforming experimental and modeling". *Catal Today* 2003; **82**:127–39".
18. "Lindberg J, Hermansson R. "Modification of reaction rate parameters for combustion of methane based on experimental investigation at furnace-like conditions". 2004, pp 1482–1484".
19. "Lindsay AL, Bromley LA. "Thermal conductivity of gas mixtures". *Ind Eng Chem* 1950; 42:1508".
20. Ma L, Trimm DL. "The design and testing of an autothermal reactor for the conversion of light hydrocarbons to hydrogen I. The kinetics of the catalytic oxidation of light hydrocarbons". *Appl Catal A* 1996; **138**: 275–83.
21. Madia GS, Barbieri G, Drioli E. "Theoretical and experimental analysis of methane steam reforming in a membrane reactor". *Can J Chem Eng*. 1999; **77**: 698–706.
22. Patel KS and Sunol AK. "Modeling and simulation of methane steam reforming in a thermally coupled membrane reactor" *International Journal of Hydrogen Energy*; **32**: 2007, 2344-58.
23. Pena MA, Gomez JP, Fierro JLG. "New catalytic routes for syngas and hydrogen production. *Appl Catal A* 1996; **144**: 7–57.
24. Rosa M. Quinta F, Manuela M Marquesa, Miguel F Baboa and Alirio E. "Modelling of the methane steam reforming reactor with large-pore catalysts". Volume **47**, Issues 9-11, 8 June 1992, Pages 2909-2914.
25. Rostrup-Nielsen JR. In: Anderson JR, Boudart M, editors. Catalysis, science and technology, Catalytic steam reforming, vol. **5**. Berlin: Springer; 1984.
26. Seader JD, Henley EJ. "Separation process principles". New York: Wiley; 1997.
27. Shu J, Grandjean S, Kaliaguine S. Methane steam reforming in asymmetric Pd and Pd–Ag/porous SS membrane reactor. *Appl Catal A* 1994;119:305–25.
28. Tsuru T, Tomohisa Y, Asaeda M. "Methane steam reforming by microporous catalytic membrane reactors". *AIChE J* 2004; 50(11): 2794–805.

29. Votruba J, Sinkule J, Hlavacek J, Skrivanek J. " Heat and mass transfer in honeycomb catalyst" *I. Chem Eng Sci* 1975;30:117–23.
30. Xu J, Froment GF. "Methane steam reforming, methanation and water-gas shift, I. Intrinsic kinetics". *AIChE J* 1989;35(1):88–96.
31. Takeguchi T, Furukawa SN, Inoue M and Eguchi K; "Autothermal reforming of methane over Ni catalysts supported over CaO–CeO_2 –ZrO_2 solid solution" *Applied Catalyst A*: General 240 (2003), 223-33.
32. Zahedi M, Rowshanzamir S Eikani MH. "Autothermal reforming of methane to synthesis gas: Modeling and simulation". Volume **34**, Issue 3, February 2009, Pages 1292-1300.
33. Wang, W., Zhu, C. and Cao, Y.; Inter. Jour. of Hydrogen Energy: 35, 2010, 1951-56.
34. Borgognoni. F., Tosti, S., Vadrucci, M. and Santucci, A.; International Journal of Hydrogen Energy, 35, 2011, 7550-7558.
35. Sun, J., Qiu, X., Wu, F., Zhu, W., Wang, W. and Hao, S.; International Journal of Hydrogen Energy, 29, 2004, 1075-81.

Appendix

For solution of PDE, a code was written in C++.

```
#include<iostream.h>

#include<conio.h>

#include<stdio.h>

#include<math.h>


int main()

{

long double Cr[5][50][100];

long double Cm[2][50][100];

long double Tr[50][100];

long double Tm[50][100];

long double Ur[50][100];

long double Pr[5][50][100];

long double Pm[2][50][100];

long double Ror[5][50][100];

long double Rr[5];

long double M[5]={2,28,16,18,44};

long double tm=0.02, tr=0.01, Sm=16.5, dt=100, dz=0.012, eps=0.33, Ji, Ep=15700, Qo=6.33e-11, tau=0.9, P, f, dp=0.00018, Rg=8.3144621;

long double Qr,R1,R2,R3;

long double k1,k2,k3,K1,K2,K3,Kco,Kh2,Kch4,Kh2o;

long double A=34.31,B=0.005469;

long double Hco,Hco2,Hh2o,Hh2,Hch4;

long double Um=3,del=1,Cpr,Cpm,hrm=2.4,pr,pm;
```

```
for(int a=0;a<50;a++)
{
        for(int b=0;b<10;b++)
        {
          k1=(1000/3.6)*9.048e10*exp(-2.095e5/(Rg*Tr[a-1][b]));
          k2=(1000/3.6)*5.43e05*exp(-7.02e4/(Rg*Tr[a-1][b]));
          k3=(1000/3.6)*2.14e09*exp(-2.115e5/(Rg*Tr[a-1][b]));
          K1=5.75e12*exp(-95616.31415/(Rg*Tr[a-1][b]));
          K2=0.0126*exp(1.26e-2/(Rg*Tr[a-1][b]));
          K3=7.240e10*exp(-178769.9352/(Rg*Tr[a-1][b]));
          Kch4=6.65e03*exp(-3.828e4/(Rg*Tr[a-1][b]));
          Kh2=6.12e-2*exp(82.90e3/(Rg*Tr[a-1][b]));
          Kco=823*exp(-70650/(Rg*Tr[a-1][b]));
          Kh2o=1.77*105*exp(88680/(Rg*Tr[a-1][b]));
Qr=1+Kco*Pr[1][a][b]+Kh2*Pr[0][a][b]+Kch4*Pr[2][a][b]+Kh2o*Pr[3]
[a][b]/Pr[0][a][b];


R1=(k1/pow(Pr[0][a][b],2.5))*(Pr[2][a][b]*Pr[3][a][b]-
pow(Pr[0][a][b],3)*Pr[1][a][b]/K1)/pow(Qr,2);
                R2=(k2/Pr[0][a][b])*(Pr[1][a][b]*Pr[3][a][b]-
pow(Pr[0][a][b],1)*Pr[4][a][b]/K2)/pow(Qr,2);

R3=(k3/pow(Pr[0][a][b],3.5))*(Pr[2][a][b]*pow(Pr[3][a][b],2)-
pow(Pr[0][a][b],4)*Pr[4][a][b]/K3)/pow(Qr,2);


                Rr[0]=R1/3+R2+R3/4;
                Rr[1]=R1-R2;
                Rr[2]=-R1-R3;
                Rr[3]=-R1-R2-R3/2;
```

```
                Rr[4]=R2+R3;


                Hh2==28.82*((Tr[a-1][b])-
298)+0.0000765*0.5*((Tr[a-1][b])*(Tr[a-1][b])-
298*298)*0.5+(0.000003288/3)*((Tr[a-1][b])*(Tr[a-1][b])*(Tr[a-
1][b])-298*298*298)+((-0.8698e-9)/4)*((Tr[a-1][b])*(Tr[a-
1][b])*(Tr[a-1][b])*(Tr[a-1][b])-298*298*298*298);

                Hh2o==18.2964*((Tr[a-1][b])-
298)+0.47212*0.5*((Tr[a-1][b])*(Tr[a-1][b])-298*298)-
(0.0013388/3)*((Tr[a-1][b])*(Tr[a-1][b])*(Tr[a-1][b])-
298*298*298)+((1314.2e-9)/4)*((Tr[a-1][b])*(Tr[a-1][b])*(Tr[a-
1][b])*(Tr[a-1][b])-298*298*298*298);

                Hco==28.95*((Tr[a-1][b])-298)+0.0044*0.5*((Tr[a-
1][b])*(Tr[a-1][b])-298*298)+(0.000003548/3)*((Tr[a-
1][b])*(Tr[a-1][b])*(Tr[a-1][b])-298*298*298)+((-2.22e-
9)/4)*((Tr[a-1][b])*(Tr[a-1][b])*(Tr[a-1][b])*(Tr[a-1][b])-
298*298*298*298);

                Hco2==36.11*((Tr[a-1][b])-
298)+0.0423*0.5*((Tr[a-1][b])*(Tr[a-1][b])-298*298)-
(0.00002887/3)*((Tr[a-1][b])*(Tr[a-1][b])*(Tr[a-1][b])-
298*298*298)+((7.464e-9)/4)*((Tr[a-1][b])*(Tr[a-1][b])*(Tr[a-
1][b])*(Tr[a-1][b])-298*298*298*298);

                Hch4==34.33*((Tr[a-1][b])-
298)+0.05469*0.5*((Tr[a-1][b])*(Tr[a-1][b])-298*298)-
(0.0000036/3)*((Tr[a-1][b])*(Tr[a-1][b])*(Tr[a-1][b])-
298*298*298)+((11e-9)/4)*((Tr[a-1][b])*(Tr[a-1][b])*(Tr[a-
1][b])*(Tr[a-1][b])-298*298*298*298);

                P=Pr[0][a-1][b]+Pr[1][a-1][b]+Pr[2][a-
1][b]+Pr[3][a-1][b]+Pr[4][a-1][b];

                Ji=(Qo*exp(-(Ep/(Rg*Tr[a-
1][b])))/tau)*((sqrt(pr)-sqrt(pm)));

                Cpr=22.62+0.115*Tr[a-1][b]-0.00026*pow(Tr[a-
1][b],2);

                Tr[a][b]=(dt/(A+B*Tr[a-1][b]))*((-R1-
R2)*(Hco+3*Hh2-Hch4-Hh2o)+(R1-R2)*(Hco2+4*Hh2-Hch4-2*Hco)+(-R1-
R2-R3/4)*(Hco2+Hh2-Hco-Hh2o))+(dt/(A+B*Tr[a-1][b]))*(8314*  Tr[a-
1][b]/(35*pr))*((Sm*tm*(1-del)*Ji/tr)+hrm*(Tm[a-1][b]-Tr[a-
1][b])/tr)-(dt/dz)*(1/A+(B*Tr[a-1][b]))*(4*Cpr*Ur[a-1][b]*Tr[a-
1][b]);
```

```
                Cpm=29+0.002199*Tm[a-1][b]-0.0000047*pow(Tm[a-
1][b],2);

                Tm[a][b]=(dt/(A+B*Tm[a-1][b]))*(Rg*Tm[a-
1][b]/(20*pm))*((Sm*del*Ji)+hrm*(Tr[a-1][b]-Tm[a-1][b])/tm)-
(dt/dz)*(1/A+(B*Tm[a-1][b]))*(4*Cpm*Um*Tm[a-1][b]);




                for(int i=0;i<5;i++)

                {

                        if(i==0)

                        {

                             Ji=(Qo*exp(-(Ep/(Rg*Tr[a-
1][b])))/tau)*(sqrt(Pr[i][a-1][b])-sqrt(Pm[i][a-1][b]));

                        }

                              else

                        {

                            Ji=0;

                        }


                      Cr[i][a][b]=Cr[i][a-
1][b]+(dt/eps)*(Ror[i][a-1][b]*Rr[i])-Ji*Sm*tm/tr-
(dt*0.5/dz)*((Cr[i][a-1][b]*(Ur[a-1][b]-Ur[a-1][b-2]))-(Ur[a-
1][b]*(Cr[i][a-1][b]-Cr[i][a-1][b-2])));

                      Pr[i][a][b]=Rg*Tr[a][b]*Cr[i][a][b];


Ror[i][a][b]=M[i]*Pr[i][a][b]/(Rg*Tr[a][b]);

                      printf("%e %e",Cr[i][a][b]);

                      printf("\t",Cr[i][a][b]);

                }

                printf("\n");

                for(int i=0;i<2;i++)
```

```
                {
                        if(i==0)
                        {
                             Ji=(Qo*exp(-(Ep/(Rg*Tr[a-
1][b])))/tau)*(sqrt(Pr[i][a-1][b])-sqrt(Pm[i][a-1][b]));
                        }
                          else
                        {
                            Ji=0;
                        }
                       Cm[i][a][b]=(-Ji*Sm*tm/tr-((Ur[a-1][b-
1]*Cm[i][a-1][b-1]-Ur[a-1][b]*Cm[i][a-1][b])*eps/dz))*dt/eps;
                       Pm[i][a][b]=Rg*Tr[a][b]*Cm[i][a][b];
                        }


                P=Pr[0][a-1][b]+Pr[1][a-1][b]+Pr[2][a-
1][b]+Pr[3][a-1][b]+Pr[4][a-1][b];


                f=1.75*(1-eps)*Ror[5][50][100]*Ur[a-1][b]*Ur[a-
1][b]/(eps*dp);
                Ur[a][b]=-f*dz/(Ur[a-1][b]*P)+Ur[a-1][b];


        }
        printf("\n");
        }
    getch();
    return 0;
}
```